

"This accepted author manuscript is copyrighted and published by Elsevier. It is posted here by agreement between Elsevier and MTA. The definitive version of the text was subsequently published in [Physics of the Earth and Planetary Interiors, Volume 239, Pages 2–13, February 2015, doi:10.1016/j.pepi.2014.06.002]. Available under license CC-BY-NC-ND."

1 **ISC-GEM: Global Instrumental Earthquake Catalogue**
2 **(1900-2009), II. Location and Seismicity Patterns**

3 I. Bondár¹, E. Robert Engdahl², A. Villaseñor³, James Harris¹, and D. Storchak¹

4 1) International Seismological Centre, UK.

5 2) University of Colorado at Boulder, USA.

6 3) Institute of Earth Sciences Jaume Almera, Spain.

7 Corresponding Author: István Bondár, istvan@isc.ac.uk

8 **Abstract**

9 We present the final results of a two-year project sponsored by the Global Earthquake
10 Model (GEM) Foundation. The ISC-GEM global catalogue consists of some 19
11 thousand instrumentally recorded, moderate to large earthquakes, spanning 110 years
12 of seismicity. We relocated all events in the catalogue using a two-tier approach. The
13 EHB location methodology (Engdahl et al., 1998) was applied first to obtain
14 improved hypocentres with special focus on the depth determination. The locations
15 were further refined in the next step by fixing the depths to those from the EHB
16 analysis and applying the new International Seismological Centre (ISC) location
17 algorithm (Bondár and Storchak, 2011) that reduces location bias by accounting for
18 correlated travel-time prediction error structure. To facilitate the relocation effort,
19 some one million seismic P and S wave arrival-time data were added to the ISC
20 database for the period between 1904 and 1970, either from original station bulletins
21 in the ISC archive or by digitizing the scanned images of the International

22 Seismological Summary (ISS) bulletin (Villaseñor and Engdahl, 2005; 2007).
23 Although no substantial amount of new phase data were acquired for the modern
24 period (1964-2009), the number of phases used in the location has still increased by
25 three millions, owing to fact that both the EHB and ISC locators use most well-
26 recorded *ak135* (Kennett et al., 1995) phases in the location.

27 We show that the relocation effort yielded substantially improved locations,
28 especially in the first half of the 20th century; we demonstrate significant
29 improvements in focal depth estimates in subduction zones and other seismically
30 active regions; and we show that the ISC-GEM catalogue provides an improved view
31 of 110 years of global seismicity of the Earth. The ISC-GEM Global Instrumental
32 Earthquake Catalogue represents the final product of one of the ten global
33 components in the GEM program, and is available to researchers at the ISC
34 (www.isc.ac.uk) website.

35 **Introduction**

36 We describe the two-year effort to produce a global instrumental catalogue for the
37 Global Earthquake Model project (GEM, www.globalquakemodel.org). The GEM
38 Foundation is a public-private partnership that drives a collaborative effort aimed at
39 developing and deploying tools and resources for earthquake risk assessment
40 worldwide. The ISC-GEM Global Instrumental Catalogue represents one of the global
41 components of the GEM project and consists of 18,809 large and moderate
42 earthquakes that have occurred during the 110-year period between 1900 and 2009.

43 In the past, several earthquake catalogues were produced with the aim of documenting
44 earthquakes that have occurred during the era of instrumental seismology (e.g. Abe,

45 1981, 1984; Abe and Noguchi, 1983a, 1983b; Gutenberg and Richter, 1954; Båth and
46 Duda, 1979; Utsu, 1979, 1982a, 1982b; and Pacheco and Sykes, 1992). The most
47 recent comprehensive catalogue is the Centennial Catalogue (Engdahl and Villaseñor,
48 2002) that covers the period 1900-2008. However, even the Centennial Catalogue is
49 inhomogenous in the sense that not all earthquakes were relocated and the earthquake
50 magnitudes were not recalculated.

51 The motivation of this project was to produce a comprehensive catalogue of large and
52 moderate earthquakes for the entire instrumental period where each earthquake is
53 relocated with the same location procedures; body and surface wave magnitudes are
54 recalculated using the original amplitude-period measurements; and finally, each
55 earthquake is characterized by either a direct measurement of M_W , or an M_W proxy
56 estimate based on non-linear regressions between M_S - M_W and m_b - M_W . Such a global
57 instrumental catalogue produced by uniform procedures would serve as input for the
58 global seismic hazard and risk components of the GEM project.

59 To achieve this goal, we manually entered a substantial number of phase arrival times,
60 and amplitude-period data from the original station bulletins in the ISC archive. We
61 also added phase arrival time data from digitally available sources that were not
62 already in the ISC database. The general overview of the project is given in Storchak
63 et al. (2014); the data collection effort is described in detail in Di Giacomo et al.
64 (2014a); and the procedures for computing body and surface wave magnitudes, as
65 well as the derivation of the nonlinear regression relations are discussed in Di
66 Giacomo et al. (2014b). In this paper we focus on the ISC-GEM location procedures
67 and results.

68 **Data**

69 Due to limitations in resources, time and data availability, we introduced time-varying
70 magnitude cut-offs for the earthquakes to be included in the ISC-GEM catalogue. For
71 the earliest instrumental period (1900-1917) the decisive factor of including events
72 was data availability due to the sparse distribution of seismological stations in the
73 global network. In the early instrumental period (1918-1959) many more
74 seismological stations were deployed but, except for a fraction of digitally available
75 data, most of the phase arrival time data still had to be entered manually. Thus, for
76 this period the available resources and time represented major limitations. For the
77 modern instrumental period (1960-2009) the vast majority of phase arrival time data
78 was already in the ISC database. With these limiting factors in mind, we set the
79 magnitude cut-offs below for the ISC-GEM event selection.

- 80 • 1900-1917: $M_S \geq 7.5$ worldwide, as well as a selection of shallow events ($M_S \geq$
81 6.5) in stable continental areas;
- 82 • 1918-1959: $M_S \geq 6.25$;
- 83 • 1960-2009: $M_S \geq 5.5$.

84 The ISC came into existence in 1964, and all data that have ever been published in the
85 ISC bulletin are stored in the ISC database. Between 1918 and 1964 the major data
86 source is the ISS (the predecessor of ISC) bulletin. Villaseñor and Engdahl (2007)
87 have already relocated earthquakes in the ISS bulletin during the period 1960-1963
88 and thus the phase data were available in the ISC database. The ISC and the ISS
89 bulletins in the ISC database provided 11 million and 330,000 phase picks for the

90 ISC-GEM events, respectively. For the period 1900-1959, the ISC database contained
91 no phase arrival time data at all.

92 To fill in the gap we added some 230,000 phase picks from the Shannon tapes - the
93 partially digitized ISS bulletin data between 1918 and 1942 owing to the initiative of
94 the first two directors of the ISC, Pat Willmore and Edouard Arnold. The Japan
95 Meteorological Agency (JMA) made its early instrumental bulletin between 1923-
96 1970 available to us and it yielded some 270,000 picks from 230 stations for events in
97 the ISC-GEM catalogue. The entire ISS bulletin (1918-1963) has been scanned by
98 Storia Geofisica Ambiente, Bologna, Italy in the frame of the Euroseismos project
99 (www.storing.ingv.it/es_web). For events for which phase picks were not already
100 digitally available we used optical character recognition software to digitize the
101 scanned ISS bulletin pages. This effort resulted in some 400,000 phase picks between
102 1918 and 1959.

103 The rest of the phase arrival data were added manually. The British Association for
104 the Advancement of Science (BAAS, predecessor of the ISS) bulletins yielded 3,800
105 picks for the period 1913-1917; the Gutenberg notepads (1904-1917) and the
106 International Seismological Association (ISA, 1904-1907) provided 1,900 phase
107 picks. Further 270,000 phase picks from 90 stations between 1904 and 1970 were
108 manually entered into the database directly from original stations bulletins collected
109 in the ISC archives.

110 For the period 1900-1903 no sufficient volume of reliable parametric station data
111 were found to allow standard relocation and magnitude estimation. Hence the
112 hypocentre parameters of earthquakes during this period were adopted from Abe and
113 Noguchi (1983a; 1983b).

114 Erroneous station coordinates may adversely affect earthquake location results. To
115 avoid this pitfall, we conducted a rigorous joint review of station parameters
116 (coordinates and elevations) using ISC, U.S. Geological Survey, National Earthquake
117 Information Center (NEIC) and U.S. Department of Energy, Lawrence Livermore
118 National Laboratory (LLNL) source materials, largely for those stations that have
119 reported to the ISC from 1964 to the present. Most inconsistencies have been resolved
120 and new revised lists of station parameters and alternate station codes have been
121 created for EHB and ISC implementation. A new feature of the station list is the
122 addition of time periods over which the station parameters are valid, including many
123 entries of stations with identical station codes but with different operational time
124 periods.

125 **Earthquake Relocation**

126 In order to obtain improved locations for the ISC-GEM catalogue over the period
127 1904-2009, we follow a two-tier procedure using the EHB (Engdahl et al., 1998) and
128 the ISC (Bondár and McLaughlin, 2009a; Bondár and Storchak, 2011) location
129 algorithms. Both the EHB and ISC location algorithms use most well-recorded
130 reported phases in line with the IASPEI standard (Storchak et al., 2003 and 2011)
131 with a valid *ak135* (Kennett et al., 1995) 1D travel-time prediction in the location,
132 together with elevation, ellipticity (Dziewonski and Gilbert, 1976; Kennett and
133 Gudmundsson, 1996; Engdahl et al., 1998), and depth-phase bounce point corrections
134 (Engdahl et al., 1998). The application of two single-event location algorithms
135 currently in use for global earthquake location provides the necessary quality
136 assurance to produce highly accurate event locations for the ISC-GEM catalogue.

137 For the early instrumental period (1904-1963) where the ISC-GEM data collection
138 effort provided data from the scanned ISS bulletins (Villaseñor and Engdahl, 2005;
139 2007), original station reports from the ISC archives and the Gutenberg notepads, we
140 obtain the initial estimates of event hypocentres using the new ISC location algorithm.
141 For the modern instrumental period (1964-2009) where no substantial volume of
142 station readings has been added to the ISC database, we simply use the preferred
143 solution from the ISC bulletin.

144 Using the initial ISC locations described above, the locations and depths of all events
145 included in the ISC-GEM catalogue are first determined using the EHB algorithm. In
146 the absence of depth constraint by local station phase data, the EHB algorithm
147 provides a comprehensive analysis of reported phases that can significantly improve
148 event depth estimates by identifying and utilizing near-event surface reflections
149 (depth phases). The new ISC location algorithm is used next with earthquake depths
150 fixed to those from the EHB analysis. The ISC algorithm provides independent depth
151 confirmation using depth phase stacking and also provides more accurate hypocentre
152 locations by taking correlated travel-time prediction error structure into account.

153 **Earthquake depth determination**

154 Depth phases provide important constraints on event depth because their travel time
155 derivatives with respect to depth are opposite in sign to those of the direct P phase.
156 Depth to origin time trade-off is also avoided by the inclusion of depth phases. These
157 phases are commonly reported as pP or sP (a P-wave or S-wave reflecting off of a
158 hard rock interface, respectively) or as pwP (a P-wave reflected off the ocean or ice
159 surface). However, as often as not these phases are simply reported as unidentified
160 phase arrival times. With knowledge of an event depth and distance, potential depth
161 phase arrivals are re-identified following each iteration in the EHB procedure using a

162 probabilistic association algorithm. Probability density functions (PDF) for depth
163 phases and the PcP phase, centered on their theoretical relative travel times for a
164 given hypocenter, are compared to the observed phase arrivals. When PDFs overlap
165 for a particular depth phase, phase identification is assigned in a probabilistic manner
166 based on the relevant PDF values, making sure not to assign the same phase to two
167 different arrivals. This procedure works relatively well in an automatic fashion, but
168 the phase identifications can depend heavily on the starting depth, which in most
169 cases is not well known. Hence, depth phase identifications for every event in the
170 ISC-GEM catalogue have been manually scrutinized for the possibility of an
171 erroneous local minimum in depth because of a poor starting depth and adjusted
172 accordingly. Normally, at least five corroborating depth phases are necessary for an
173 EHB depth to be accepted.

174 In order to determine pwP arrival times and correct all depth phases for topography or
175 bathymetry at their reflection points on the earth's surface, it is necessary to first
176 determine the latitude and longitude of these bounce points and then the
177 corresponding seafloor depth or continental elevation. Bounce point coordinates are
178 easily computed from the distance, azimuth and ray parameter of the depth phase (pP
179 in the case of pwP). The NOAA ETOPO1 global relief file (Amante and Eakins,
180 2009) was averaged over 5 x 5 minute equal area cells and then projected on a 5 x 5
181 minute equi-angular cell model using a Gaussian spatial filter. The use of a smoothed
182 version of ETOPO1 is justified because the reflection of a depth phase does not take
183 place at one single point, but over a reflection zone with a size determined by the
184 Fresnel zone of the wave. The maximum half width of a ray with a wavelength of 10
185 km and a ray path length of 1000 km is estimated to be 36 km (Nolet, 1987). The
186 topographic and bathymetric information in this version of ETOPO1, with elevations

187 referred to land or sea bottom, is used to determine the correction for bounce point
188 elevation/depth, which is added to the computed travel times for depth phases.
189 Theoretical times are not computed for pwP phases in the case of bounce point water
190 depths ≤ 1.5 km because it is nearly impossible to separate the pP and pwP arrivals on
191 most records (about 2s separation).

192 Despite the general success of the EHB procedures for depth determination, there
193 remain some issues that must be taken into account. For example, the relative
194 frequency (or amplitude) of depth phase observations is sensitive to local structure at
195 bounce points. Many depth phases reflect in the vicinity of plate boundaries where the
196 slopes of surface reflectors are large (> 1 degree). Reflections at a dipping reflection
197 zone may lead to small asymmetries in depth phase waveforms and, may influence
198 their relative amplitudes, resulting in a greater potential for phase mis-identifications.
199 In addition, for short-period (1s) waves, water-sediment interfaces at the sea bottom
200 may have small impedance contrasts. Consequently, on short-period seismograms the
201 amplitude of a pwP phase may be comparable to or larger than the pP phase reflecting
202 at the sea bottom, and pwP may easily be mis-identified as pP.

203 One outstanding issue is that for large shallow-focus complex earthquakes pP often
204 arrives in the source-time function of the P phase, which may consist of one or more
205 sub-events. The gross features of the source-time functions of P and pP, however,
206 remain discernible in broadband displacement records and the exact onset times of
207 depth phases can be further refined by examination of velocity seismograms that are
208 sensitive to small changes in displacement. For the GEM project we have relied
209 primarily on reported phase arrival times, usually read from short-period
210 seismograms. However, for large complex events EHB depths ordinarily have to be

211 set to depths published by USGS/NEIC that have been determined by rigorous
212 analysis of phase arrival times read from broadband seismograms.

213 Finally, there are many events in the ISC-GEM catalogue for which there are no
214 reported depth phases or for which those that were reported are inconsistent,
215 especially in the earlier part of the 20th century. For these events a nominal depth is
216 adopted, based on the depth distribution of neighboring events that are well
217 constrained in depth and are consistent with other event depths in that tectonic setting.
218 For every subduction zone worldwide, all ISC-GEM events were plotted in cross
219 section with respect to the arc center of curvature to assist in setting depths of those
220 events that have no other available depth constraints.

221 **Earthquake epicentre and origin time determination**

222 In the next step of ISC-GEM location procedures we determine the earthquake
223 epicenter and origin time parameters by fixing the depth to that obtained from the
224 EHB analysis. The EHB location and origin time are used as the initial guess for the
225 ISC locator. The ISC location algorithm can further refine the locations because it
226 reduces the location bias introduced by the correlated travel-time prediction error
227 structure due to unmodeled 3D heterogeneities in the Earth.

228 Figure 1 shows the total number of associated phases and those that are used in the
229 location in each year. As the number of phases increases almost exponentially in time,
230 the number of phases traveling along similar ray paths increases accordingly,
231 contributing more and more to the potential location bias. Thus, accounting for the
232 correlated error structure becomes imperative.

233 Figure 2 compares deviations between the EHB and corresponding ISC locations for
234 events in the ISC-GEM catalogue. The median location difference is 9 km, that is,

235 50% of the locations are within 9km of each other. Furthermore, 90% of the location
236 differences are less than 20 km. Given that the ISC-GEM catalogue locations are
237 predominantly teleseismic, the EHB and ISC locations show remarkable consistency.
238 Figure 2b shows the location deviations with respect to the EHB locations. The plot
239 indicates that there is no bias between the EHB and ISC locations.

240 Even though the depth is fixed to the EHB depth, the ISC location algorithm may
241 obtain an independent depth estimate through the depth-phase stacking (Murphy and
242 Barker, 2006) provided that sufficient number of first-arriving P and depth-phase
243 pairs are available. Some 65% of the events in the ISC-GEM catalogue also have
244 depth estimates from the depth phase stacking. Figure 3 shows an excellent agreement
245 between the depths obtained through the EHB depth determination procedures and the
246 depth-phase stacking.

247 **Uncertainty estimates**

248 Accounting for correlated errors not only reduces location bias, but also provides
249 more accurate uncertainty estimates. Most location algorithms assume independent,
250 normally distributed observational errors. Unfortunately, this assumption rarely holds
251 because the 1D global average velocity model used in the location does not capture all
252 the 3D velocity heterogeneities and travel-time predictions along similar ray paths
253 become correlated, decreasing the effective number of degrees of freedom. Because
254 the number of independent observations is less than the total number of observations
255 used in the location, the assumption of independence inevitably leads to
256 underestimated uncertainty estimates. Since the ISC location algorithm uses the
257 effective number of degrees of freedom, the formal location uncertainties described
258 by the *a posteriori* model covariance matrix become larger, resulting in enlarged and
259 more circular error ellipses. Figure 4 shows the distribution of origin time uncertainty

260 and the area of the error ellipse, both scaled to the 90% confidence level. The median
261 origin time uncertainty is 0.25s and the median area of the error ellipse is 105 km².

262 Because the depth is fixed to the EHB depth, no formal depth uncertainties can be
263 calculated by the ISC locator. In order to provide a depth uncertainty, we use the
264 depth-phase depth uncertainty from the depth phase stacking, if available. These are
265 typically the events where the EHB depth determination procedures relied on the
266 reported depth phases. If no depth-phase stack exists for an event we estimate the
267 depth uncertainty as the median absolute deviation of the depths in the corresponding
268 ISC default depth grid cell if it exists, otherwise we set the depth uncertainty to a
269 nominal 25 km. Note that the ISC default depth grid cells are only defined if there are
270 sufficient number of observations with a limited 25 to 75 percentile range (see Bondár
271 and Storchak, 2011); therefore the median absolute deviation of the depths in a grid
272 cell is typically smaller than 15 km.

273 Besides the formal location uncertainty estimates, measures of the network geometry
274 may also indicate the quality of the location. Figure 5 shows the cross-plot of
275 secondary azimuthal gap and the eccentricity of the error ellipse for all candidate
276 events processed for the ISC-GEM catalogue. The secondary azimuthal gap is defined
277 as the largest azimuthal gap filled by a single station (Bondár et al., 2004). The
278 eccentricity varies between 0 and 1; at zero eccentricity the error ellipse becomes a
279 circle, indicating evenly distributed stations around the event, while the error ellipse
280 degenerates to a line at a unit eccentricity, indicating that all stations aligned at a
281 single azimuth from the event.

282 We consider events having the most accurate locations as those that are recorded with
283 a secondary azimuthal less than 120° and with an error ellipse eccentricity less than

284 0.75, or those that qualify for GT5 candidate (Bondár and McLaughlin, 2009b). Out
285 of the 19,711 earthquakes that we have processed 14,517 locations belong to this
286 category; 12,570 events also have independent depth estimates from the depth-phase
287 stacking.

288 Events recorded with a huge secondary azimuthal gap ($sgap \geq 270^\circ$) or events
289 recorded only with a small number of stations ($nsta \leq 5$) are considered unreliable
290 locations and are listed in the Supplementary of the main ISC-GEM catalogue. Note
291 that there are only 45 events relegated to the Supplementary catalogue based on the
292 location accuracy measures; the vast majority of the 903 events listed in the
293 Supplementary catalogue are there because they had an insufficient number of
294 amplitude-period observations to calculate M_S or m_b . About half of the events in the
295 Supplementary catalogue have the most accurate location and depth estimates, and
296 many of them are deep events. Thus, for studies that do not require magnitude
297 estimates, it is safe to use the locations listed in the Supplementary catalogue.

298 **Earthquake relocation results**

299 The ISC-GEM catalogue consists of 18,808 earthquakes between 1900 and 2009.
300 Apart from 10 events between 1900 and 1903, for which we adopt the hypocentre
301 parameters from the Abe catalogue (Abe, 1981, 1984; Abe and Noguchi, 1983a,
302 1983b), we relocated all earthquakes using the two-step location procedure described
303 above.

304 One of the major objectives of this project was to provide improved hypocentre
305 estimates for events in the ISC-GEM catalogue. To achieve this goal we launched an
306 ambitious data entry effort to add station readings that did not previously exist in

307 digital form. For events occurring between 1904 and 1963 some 1,200,000
308 observations were entered into the database either from the station reports in the ISC
309 archive or by digitizing the scanned images of the ISS bulletin (Villaseñor and
310 Engdahl, 2005; 2007). Of the total number of added phases some 600,000 are P-type
311 phases, 300,000 are S-type phases, and the rest are amplitude readings. Some 665,000
312 P and S type phases contributed to the relocation of events in the historical period.
313 Although no substantial amount of new phase data were acquired for the modern
314 period (1964-2009), the number of phases used in the location has still dramatically
315 increased. Recall that in the past the vast majority of locations in the ISC bulletin
316 were obtained using only first-arriving Pg, Pn and P phases. The number of defining
317 phases used in the location in the modern period increased from 5,373,783 to
318 8,323,546 owing to fact that both the EHB and ISC locators use most *ak135* phases in
319 the location.

320 Figure 6 shows the box-and-whisker plots of the median number of stations and the
321 median secondary azimuthal gap (largest azimuthal gap filled by a single station) in
322 each decade. The box in a box-and-whisker plot shows the range between first (25%)
323 and third (75%) quartiles, and the band inside the box represents the second (the
324 median) quartile. The ends of the whiskers indicate the minimum and maximum of
325 the data. As the number of stations used in the location increases with time, the
326 median secondary azimuthal gap decreases and levels off around 45°.

327 The preferred locations before the ISC-GEM project constituted a mixture of
328 locations from the Abe (Abe, 1981, 1984; Abe and Noguchi, 1983), the Centennial
329 (Engdahl and Villaseñor, 2002), the ISS (Villaseñor and Engdahl, 2005; 2007) and the
330 ISC catalogues. We compare these locations (before) to the ISC-GEM locations
331 (after). Figure 7 shows the locations before and after the ISC-GEM relocations for the

332 entire period, 1900-2009. Even at the global scale it is apparent that the earthquake
333 locations are better clustered in the ISC-GEM catalogue. In the historical period many
334 event depths were fixed to the surface; due to the better depth estimates, this artifact is
335 removed from the ISC-GEM catalogue.

336 Figure 8 shows the distributions of location and depth differences before and after the
337 ISC-GEM relocations. The median distance between the before and after locations is
338 10km. 90% of the events moved by less than 25km, and 90% of the depth changes are
339 between ± 20 km.

340 We expect that the largest differences between the before and after ISC-GEM
341 relocations will come from the early years. Figures 9-10 show the box-and-whisker
342 plots of the location, depth and origin time differences in each decade. Indeed, most
343 of the large location changes occur in the first half of the century; the effect of
344 improved depth estimates can be seen through the entire period but large variations
345 level off with time.

346 Recall that for about one-third of the events had no depth phase information, and
347 therefore their depth were fixed to a depth that is consistent with the depth of other
348 events in that particular tectonic setting. Although this carries a small risk that the
349 depth of intraplate events might have been adjusted to an interplate boundary, we
350 have by no means forced event hypocenters to occur on plate boundaries, but we had
351 rather let the data decide the best location estimate. An erroneous depth for an
352 intraplate (as a matter of fact, for any) event would generate large residuals and
353 prompted us to carry out a more involved study to get the hypocenter right. Since
354 hypocentres in the first part of the 20th century were the most vulnerable to large
355 location errors, we manually reviewed every single event occurring between 1903 and

356 1930 in the ISC-GEM catalogue as well as all other problematic events. Furthermore,
357 the quality of the event locations and depths are not only described with their formal
358 uncertainties but with qualitative flags ranging from A to D. Events with depth fixed
359 to the corresponding tectonic setting, or epicentres determined by a poor network
360 geometry are never considered the best quality and given the lowest level quality
361 flags.

362 **Conclusions**

363 The ISC-GEM Global Instrumental Catalogue represents the final product for one of
364 the global components of the GEM project. The ISC-GEM catalogue consists of
365 18,809 large and moderate earthquakes that have occurred during the 110-year period
366 between 1900 and 2009. The ISC-GEM bulletin contains some 13 million phases
367 associated with the earthquakes in the catalogue.

368 One of the requirements from the GEM project was that each event in the ISC-GEM
369 instrumental catalogue is characterized by a measure of magnitude. For a number of
370 events without a direct measure of M_W there were insufficient number of amplitude
371 measurements to calculate either m_b or M_S . Furthermore, since body wave magnitudes
372 were regularly reported only from the second half of the 20th century, many deep
373 events from the early period has no magnitude estimate and therefore cannot be
374 included in the main ISC-GEM catalogue. We felt the need to create a Supplementary
375 catalogue to the ISC-GEM catalogue that contains the 858 large earthquakes with no
376 magnitude estimates, as well as 45 events with less reliable locations. Hence, for
377 seismicity studies that do not require magnitude information, events in the
378 Supplementary catalogue can be joined with the main ISC-GEM catalogue.

379 All events (except for 10 events between 1900 and 1903) in the ISC-GEM catalogue
380 are relocated using uniform and rigorous location procedures. During the project an
381 unprecedented amount of phase arrival data were scanned, digitized and archived in
382 the ISC database. Owing to the ISC-GEM location procedures and to the substantial
383 increase in the volume of observational data used in the relocations, the ISC-GEM
384 catalogue offers an improved view of the seismicity of the Earth. The ISC-GEM
385 locations are better clustered and considerably reduce scatter in location estimates.
386 The significantly improved depth estimates provide a better resolution of earthquakes
387 associated with subducting slabs.

388 The ISC-GEM Global Instrumental Earthquake Catalogue (1900-2009) is made
389 publicly available at the ISC website, www.isc.ac.uk. The ISC-GEM catalogue is
390 regularly updated based on the feedback from researchers. The changes are
391 documented at www.isc.ac.uk/iscgem/update_log.

392 **Acknowledgements**

393 This project was sponsored by the GEM Foundation. We are grateful to Nobuo
394 Hamada (Japan Meteorological Agency, emeritus, Japan) who provided a digital copy
395 of JMA historical bulletin data for 1923-1970 and Katsuyuki Abe for making
396 available a CD-ROM with the catalogue of Abe and Noguchi. We wish to recognize
397 the initiative of the late Edouard Arnold and Pat Willmore, former Directors of the
398 ISC, for transferring a large fraction of the ISS paper bulletins onto punched cards and
399 preparing the Shannon tape. We also wish to acknowledge the effort of Tom Boyd,
400 Colorado School of Mines, USA, for his contribution in correcting the data on the

401 Shannon tape. We also thank George Helffrich, Emile Okal and an anonymous
402 reviewer for their thorough review of the manuscript.

403 **References**

- 404 Abe, K., 1981. Magnitudes of large shallow earthquakes from 1904 to 1980, *Phys.*
405 *Earth Planet. Int.*, **27**, 72-92.
- 406 Abe, K., and S. Noguchi, 1983a. Determination of magnitudes for large shallow
407 earthquakes, 1898-1917, *Phys. Earth Planet. Inter.*, **32**, 45-59.
- 408 Abe, K., and S. Noguchi, 1983b, Revision of magnitudes of large shallow earthquakes
409 1897 – 1912, *Phys. Earth Planet. Int.*, **33**, 1-11.
- 410 Abe, K., 1984. Complements to "Magnitudes of large shallow earthquakes from 1904
411 to 1983", *Phys. Earth Planet. Int.*, **34**, 17-23.
- 412 Amante, C., and B.W. Eakins, 2009. ETOPO1 1 arc-minute global relief model:
413 Procedures, data sources and analysis, *NOAA Technical Memorandum NESDIS*
414 *NGDC-24*.
- 415 Båth, M., and S.J. Duda, 1979. Some aspects of global seismicity. *Tectonophysics*, **54**,
416 T1-T8.
- 417 Bondár, I., S.C. Myers, E.R. Engdahl, and E.A. Bergman, 2004. Epicenter accuracy
418 based on seismic network criteria, *Geophys. J. Int.*, **156**, 483-496, doi:
419 10.1111/j.1365-246X.2004.02070.x.

420 Bondár, I., and K. McLaughlin, 2009a. Seismic location bias and uncertainty in the
421 presence of correlated and non-Gaussian travel-time errors, *Bull. Seism. Soc. Am.*, **99**,
422 172-193.

423 Bondár, I., and K. McLaughlin, 2009b. A new ground truth data set for seismic
424 studies, *Seism. Res. Let.*, **80**, 465-472.

425 Bondár, I., and D. Storchak, Improved location procedures at the International
426 Seismological Centre, 2011. *Geophys. J. Int.*, **186**, 1220-1244, doi:10.1111/j.1365-
427 246X.2011.05107.x.

428 Di Giacomo, D., J. Harris, A. Villaseñor, D.A. Storchak, E.R. Engdahl, W.H.K. Lee,
429 and the Data Entry Team, 2013. ISC-GEM: Global Instrumental Earthquake
430 Catalogue (1900-2009), I. Data collection from early instrumental seismological
431 bulletins, *Phys. Earth Planet. Int.*, submitted.

432 Di Giacomo, D., I. Bondár, D.A. Storchak, E.R. Engdahl, P. Bormann, and J. Harris,
433 2013. ISC-GEM: Global Instrumental Earthquake Catalogue (1900-2009), III.
434 Re-computed M_S and m_b , proxy M_W , final magnitude composition and completeness
435 assessment, *Phys. Earth Planet. Inter.*, submitted.

436 Dziewonski, A.M., and F. Gilbert, 1976. The effect of small, aspherical perturbations
437 on travel times and a re-examination of the correction for ellipticity, *Geophys. J. R.*
438 *Astr. Soc.*, **44**, 7-17.

439 Engdahl, E.R., R. van der Hilst, and R. Buland, 1998. Global teleseismic earthquake
440 relocation with improved travel times and procedures for depth determination, *Bull.*
441 *Seism. Soc. Am.*, **88**, 722-743.

442 Engdahl, E.R., and A. Villaseñor, Global Seismicity: 1900–1999, 2002. in W.H.K.
443 Lee, H. Kanamori, P.C. Jennings, and C. Kisslinger (editors), *International Handbook*
444 *of Earthquake and Engineering Seismology*, Part A, Chapter 41, 665–690, *Academic*
445 *Press*.

446 Gutenberg, B., and C. F. Richter, 1954. Seismicity of the Earth and Associated
447 Phenomena. *Princeton Univ. Press*, Princeton, N.J., 310 pp.

448 Kennett, B.L.N., E.R. Engdahl, and R. Buland, 1995. Constraints on seismic
449 velocities in the Earth from traveltimes, *Geophys. J. Int.*, **122**, 108-124.

450 Kennett, B.L.N., and O. Gudmundsson, 1996. Ellipticity corrections for seismic
451 phases, *Geophys. J. Int.*, **127**, 40-48.

452 Murphy, J.R., and B.W. Barker, 2006. Improved focal-depth determination through
453 automated identification of the seismic depth phases pP and sP, *Bull. Seism. Soc. Am.*,
454 **96**, 1213-1229.

455 Nolet, G., 1987. Seismic wave propagation and seismic tomography, in *Seismic*
456 *Tomography*, pp. 1-23, ed. Nolet, G., Reidel, Dordrecht.

457 Pacheco, J. F., and L. R. Sykes, 1992. Seismic moment catalog of large shallow
458 earthquakes, 1900 to 1989. *Bull. Seism. Soc. Am.* **82**, 1306-1349.

459 Storchak, D.A., J. Schweitzer, and P. Bormann, 2003. The IASPEI Standard Seismic
460 Phase List, *Seismol. Res. Lett.* **74**, 6, 761-772.

461 Storchak, D.A., J. Schweitzer, and P. Bormann, 2011. Seismic phase names: IASPEI
462 Standard, in *Encyclopedia of Solid Earth Geophysics*, 1162-1173, Ed. H.K. Gupta,
463 Springer.

464 Storchak, D.A., D. Di Giacomo, E.R. Engdahl, I Bondár, W.H.K. Lee and P.
465 Bormann, 2013. The ISC-GEM global instrumental earthquake catalogue (1900-
466 2009): Introduction, *Phys. Earth Planet. Inter.*, submitted.

467 Utsu, T., 1979. Seismicity of Japan from 1885 through 1925, A new catalog of
468 earthquakes of $M > 6$ felt in Japan and smaller earthquakes which caused damage in
469 Japan (in Japanese with English abstract). *Bull. Earthquake Res. Inst.* **54**, 253-308.

470 Utsu, T., 1982a. Seismicity of Japan from 1885 through 1925 (Correction and
471 supplement) (in Japanese with English abstract). *Bull. Earthquake Res. Inst.* **57**, 111-
472 117.

473 Utsu, T., 1982b. Catalog of Large earthquakes in the region of Japan from 1885
474 through 1980 (in Japanese with English abstract). *Bull. Earthquake Res. Inst.*, **57**,
475 401-463.

476 Villaseñor, A., and E.R. Engdahl, 2005. A digital hypocenter catalog for the
477 International Seismological Summary, *Seism. Res. Let.*, **76**, 554-559.

478 Villaseñor, A., and E.R. Engdahl, 2007. Systematic relocation of early instrumental
479 seismicity: Earthquakes in the International Seismological Summary for 1960-1963,
480 *Bull. Seism. Soc. Am.*, **97**, 1820-1832.

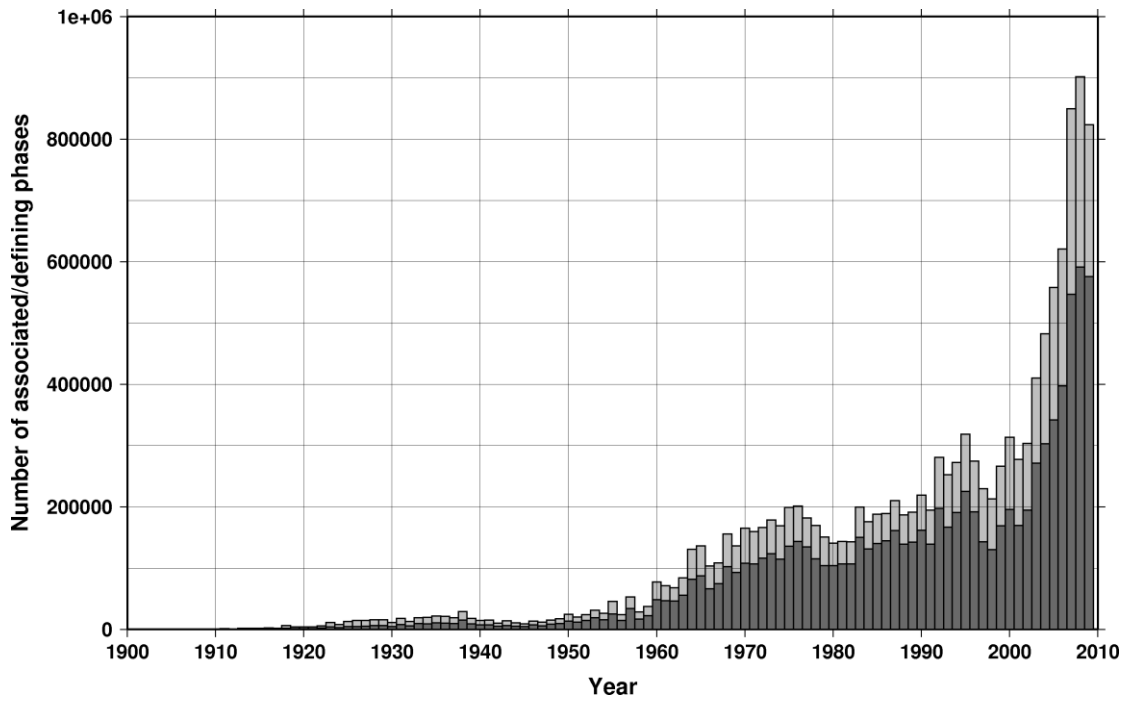
481

482

483

484

485



486

487 **Figure 1. Annual number of associated (gray) and defining (dark gray) phases in the ISC-GEM**

488 **catalogue. A defining phase is a phase that was used in the location.**

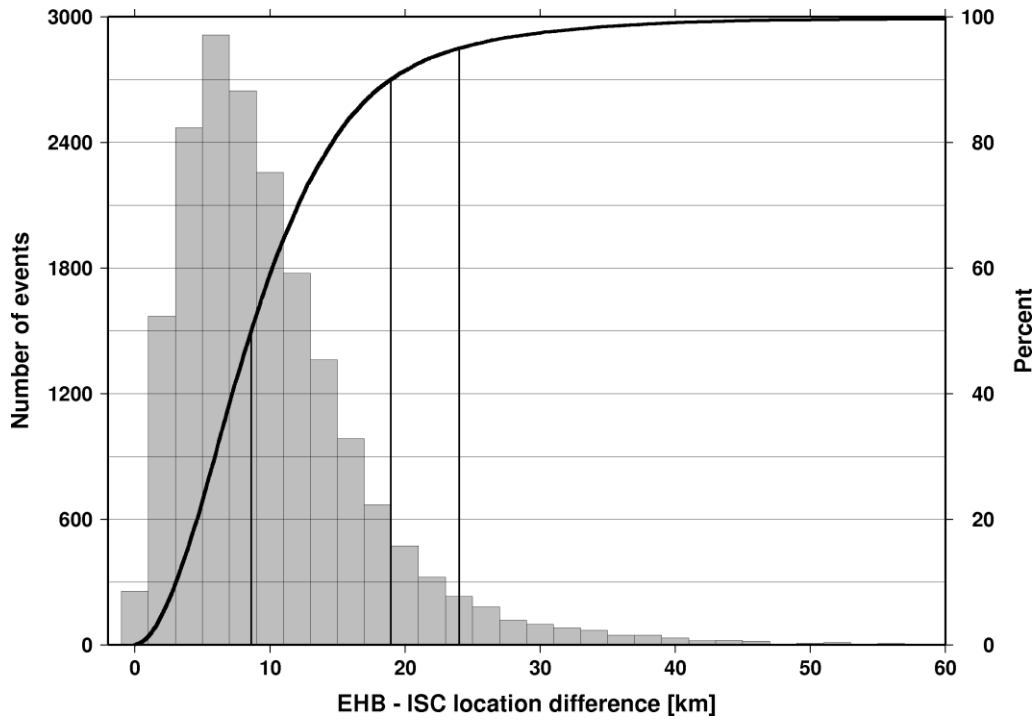
489

490

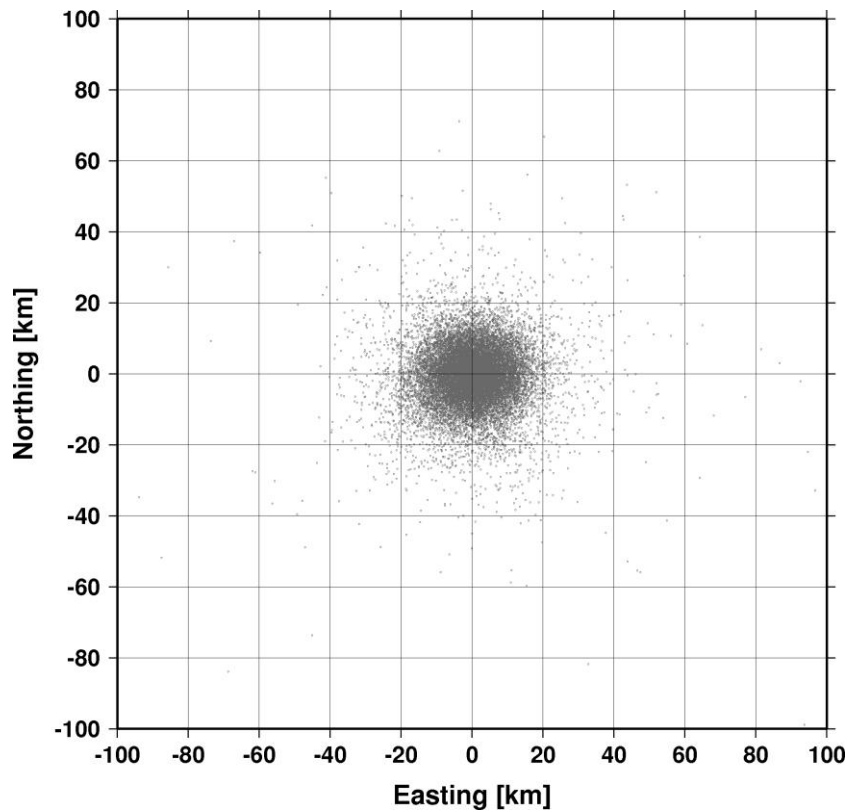
491

492

493

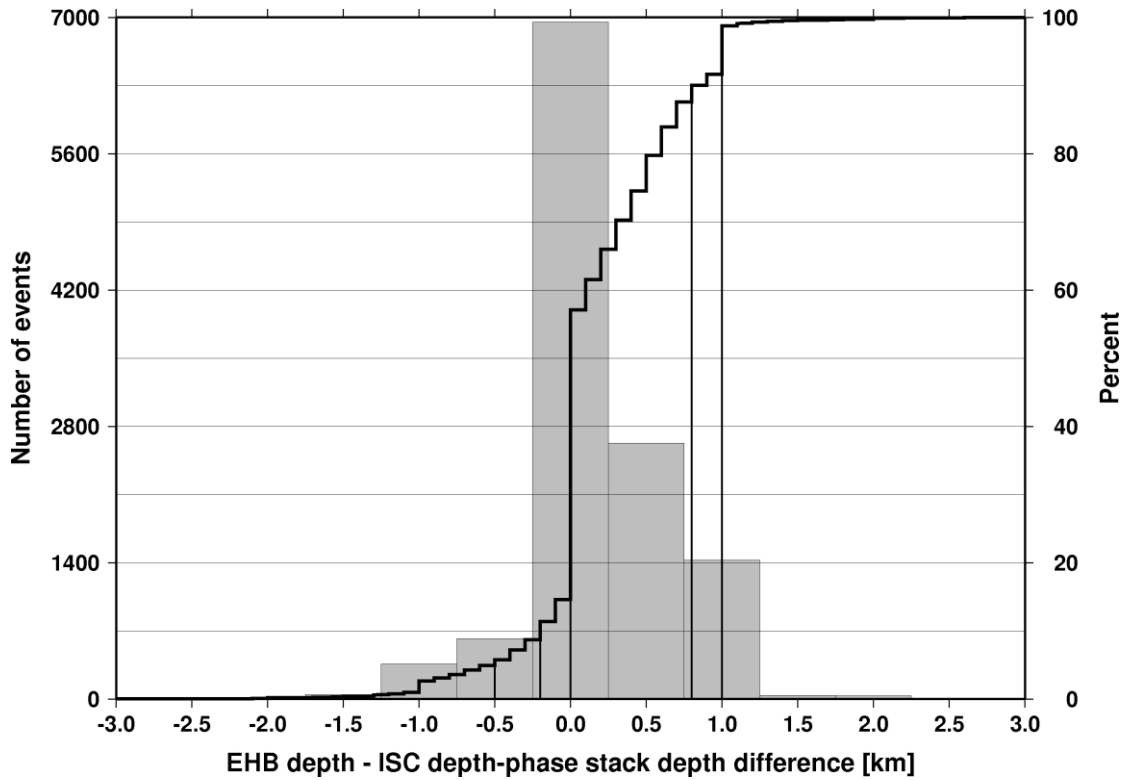


494



495

496 **Figure 2. a) Histogram of distances between the EHB and ISC locations for events in the ISC-**
 497 **GEM catalogue. The 50% (median), 90% and 95% percentile points on the cumulative**
 498 **distribution (thick line) are marked the vertical lines.. b) The deviations between the EHB and**
 499 **ISC locations show no bias.**



500

501 **Figure 3. Histogram of the difference between the depth estimates from depth phase stacking and**
 502 **the EHB depth determination. The 5%, 10%, 50%, 90% and 95% percentile points on the**
 503 **cumulative distribution (thick line) are indicated by the vertical lines.**

504

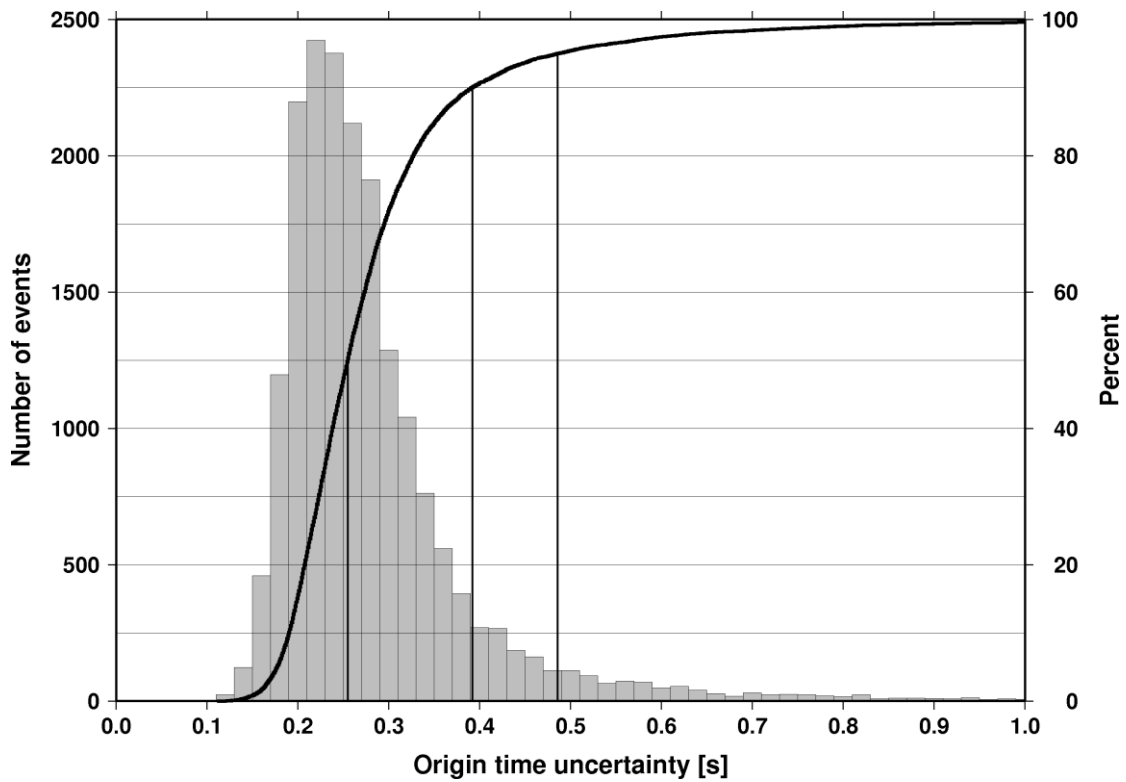
505

506

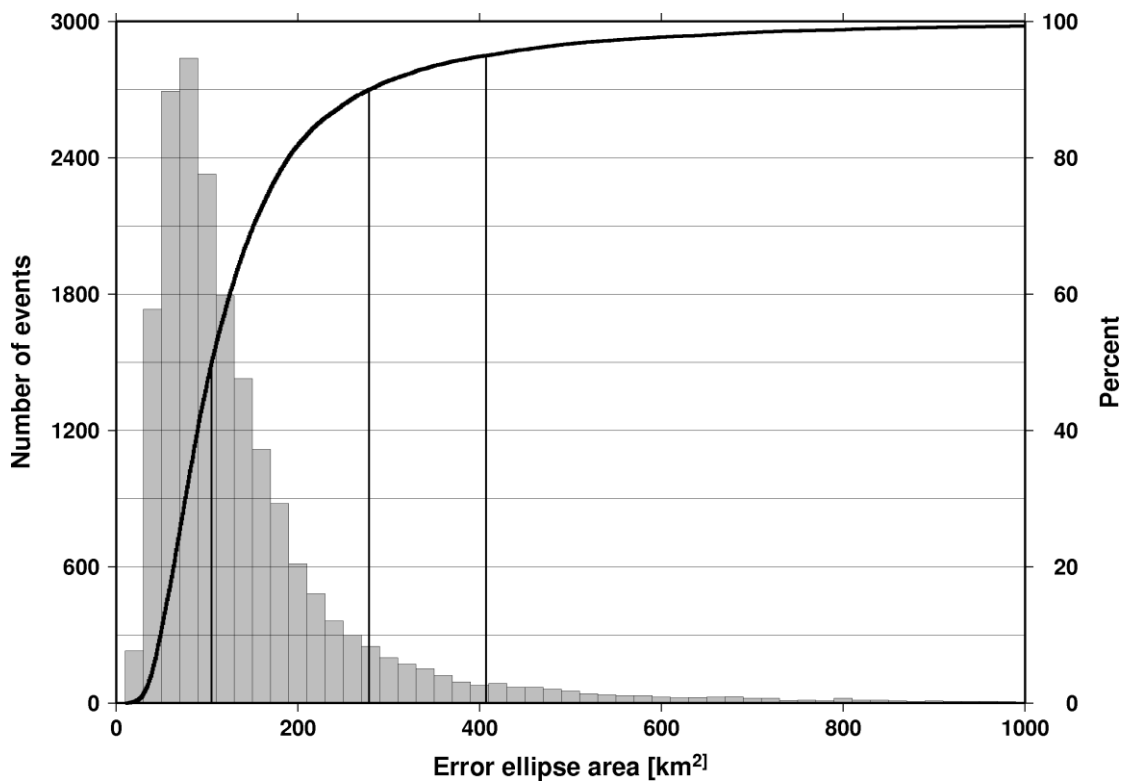
507

508

509

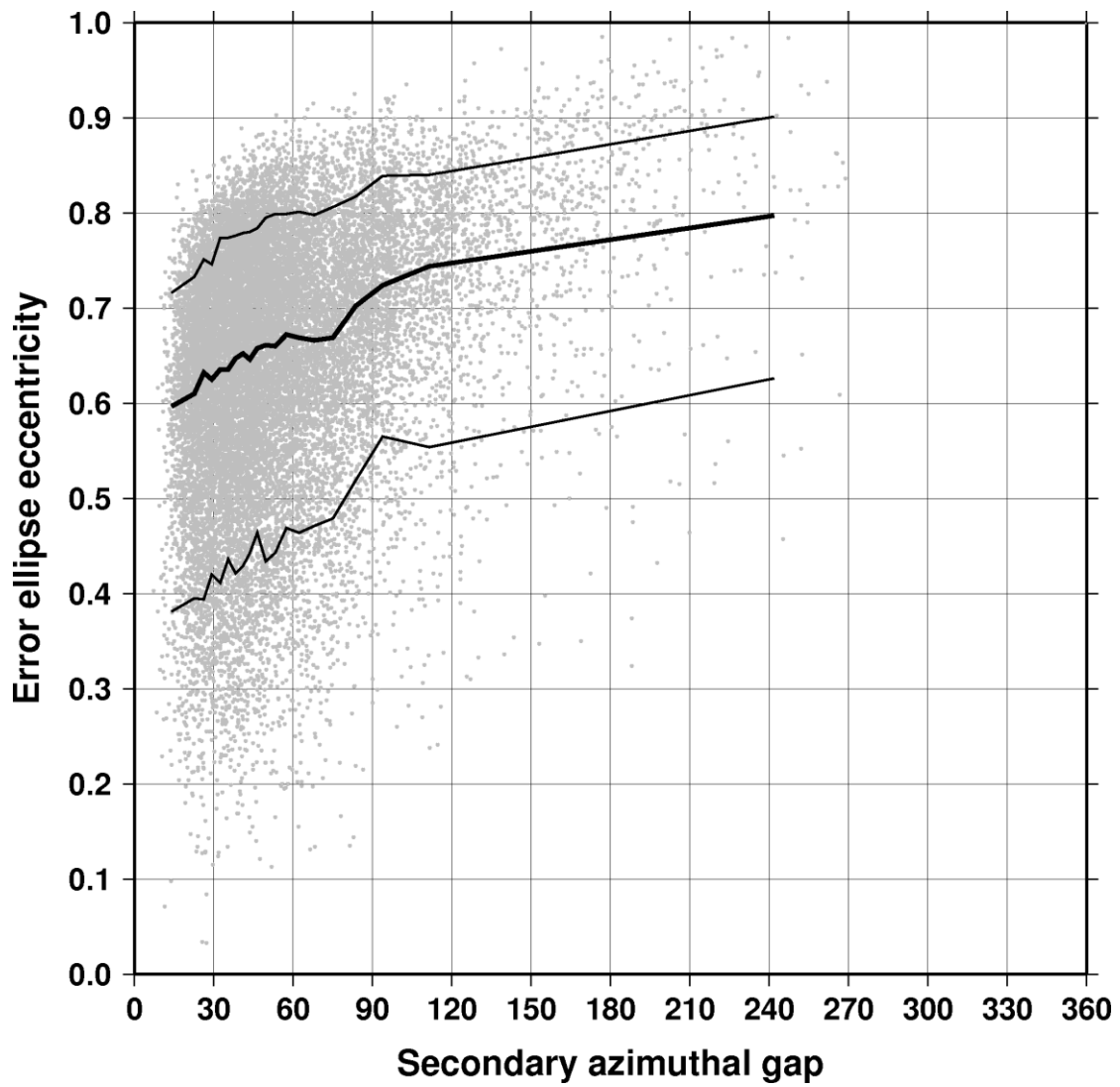


510



511

512 **Figure 4. Histograms of the a) origin time uncertainty, and b) area of the 90% confidence error**
 513 **ellipse for events in the ISC-GEM catalogue. The 50% (median), 90% and 95% percentile points**
 514 **on the cumulative distribution (thick line) are marked by the vertical lines.**



515

516 **Figure 5. Error ellipse eccentricity as a function of secondary azimuthal gap. The thick line**
517 **indicates the median curve; the 10% and 90% percentile curves are drawn by thin lines.**

518

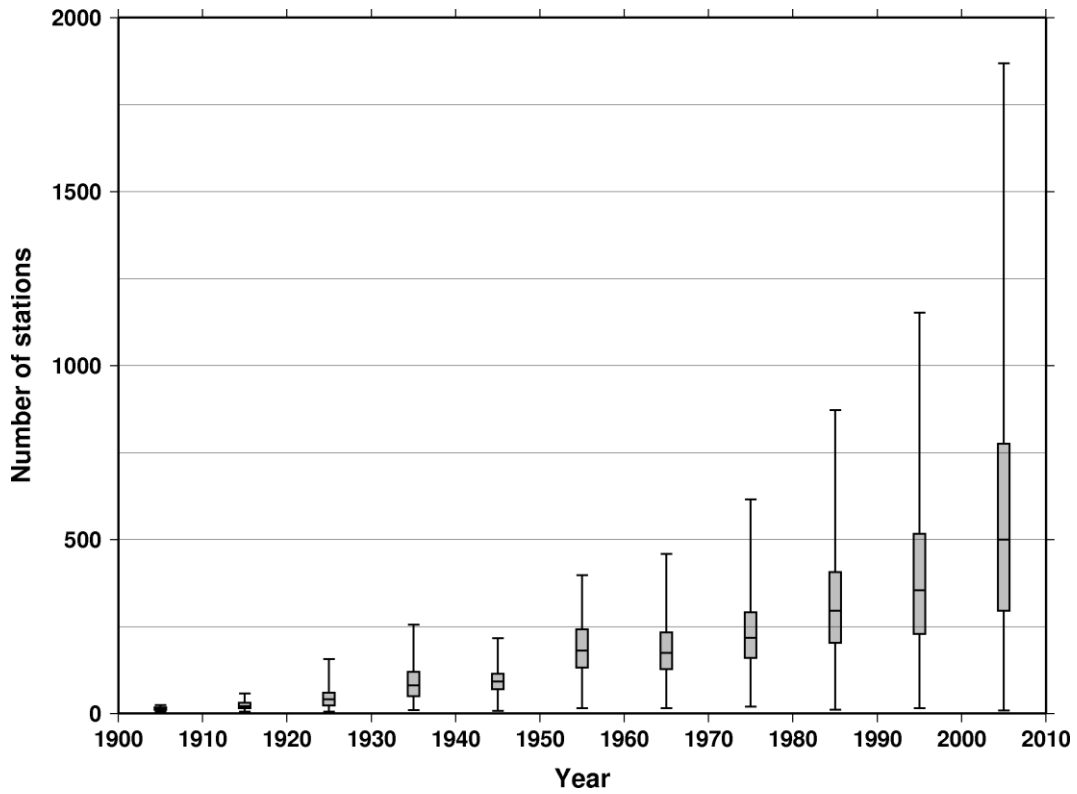
519

520

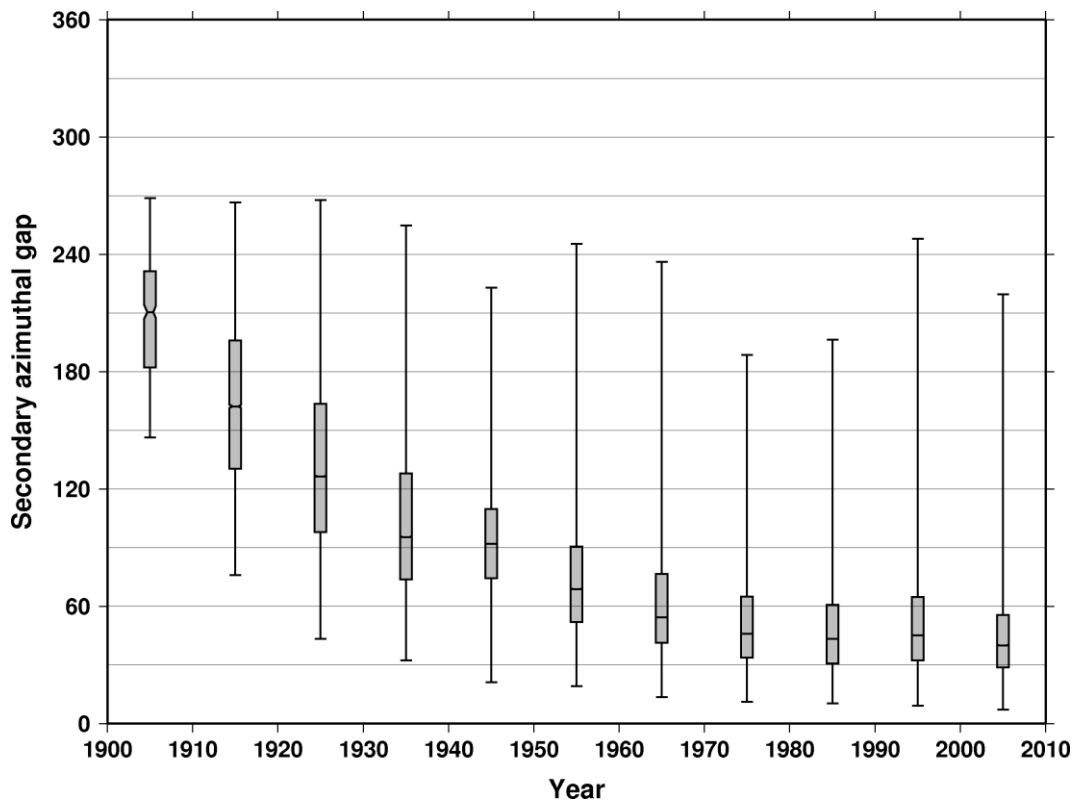
521

522

523



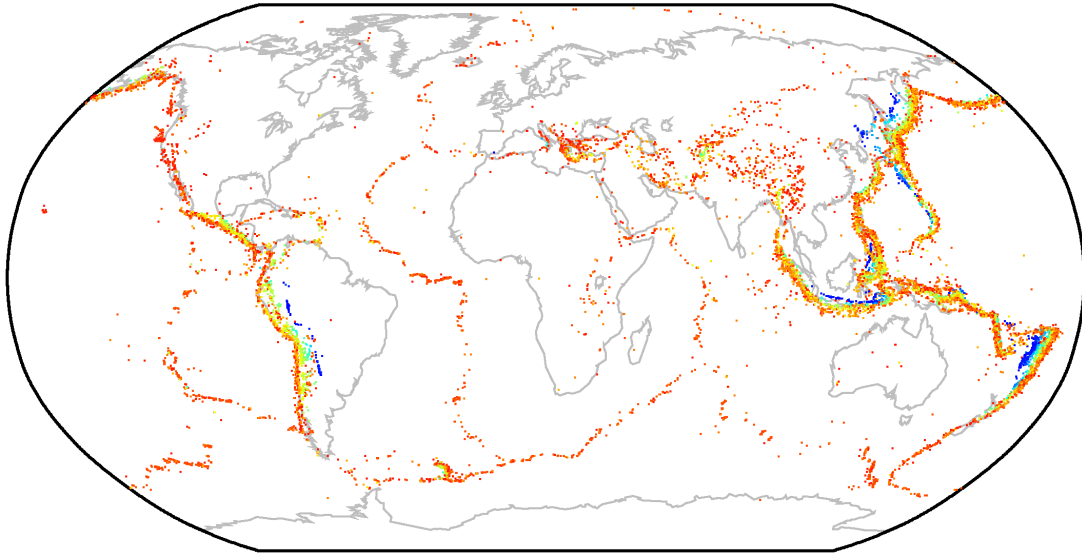
524



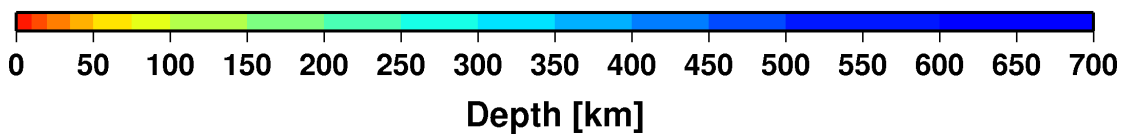
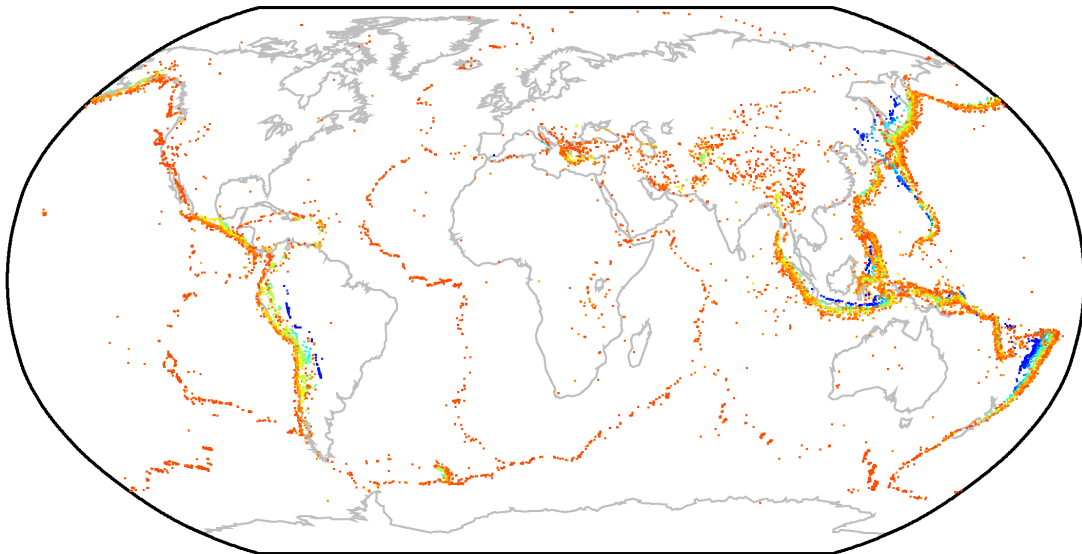
525

526 Figure 6. Box-and-whisker plot of a) the number of stations, and b) the secondary azimuthal gap
 527 in each decade. The gray boxes represent the 25% - 75% quartile ranges; the vertical extent of
 528 the lines indicate the full, minimum to maximum range.

Before



After

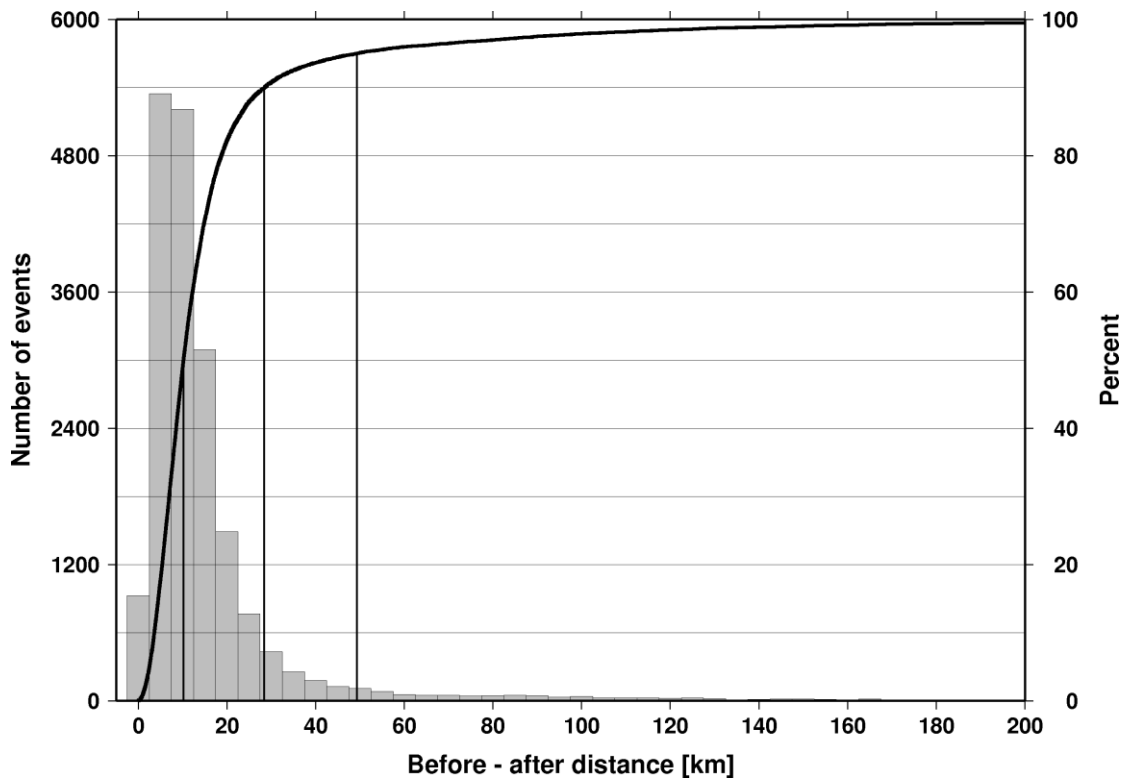


529

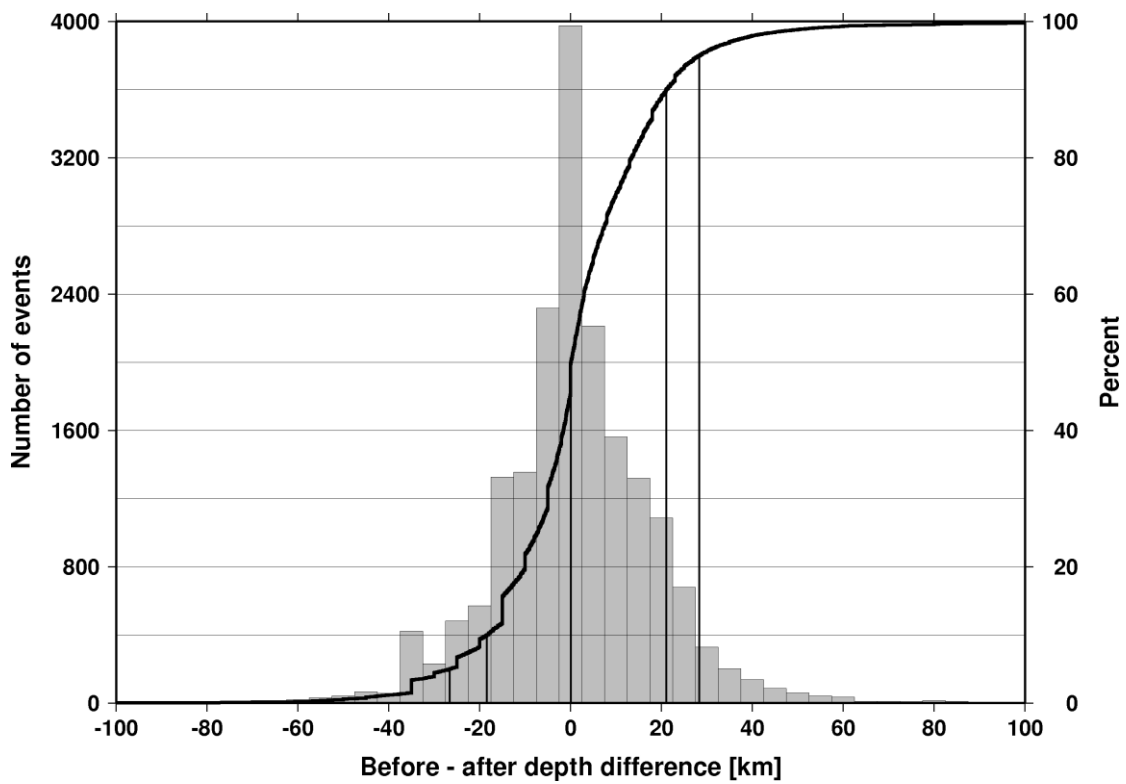
530 **Figure 7. Preferred locations before and after the ISC-GEM relocations. The ISC-GEM locations**
531 **show an improved view of the seismicity of the Earth.**

532

533

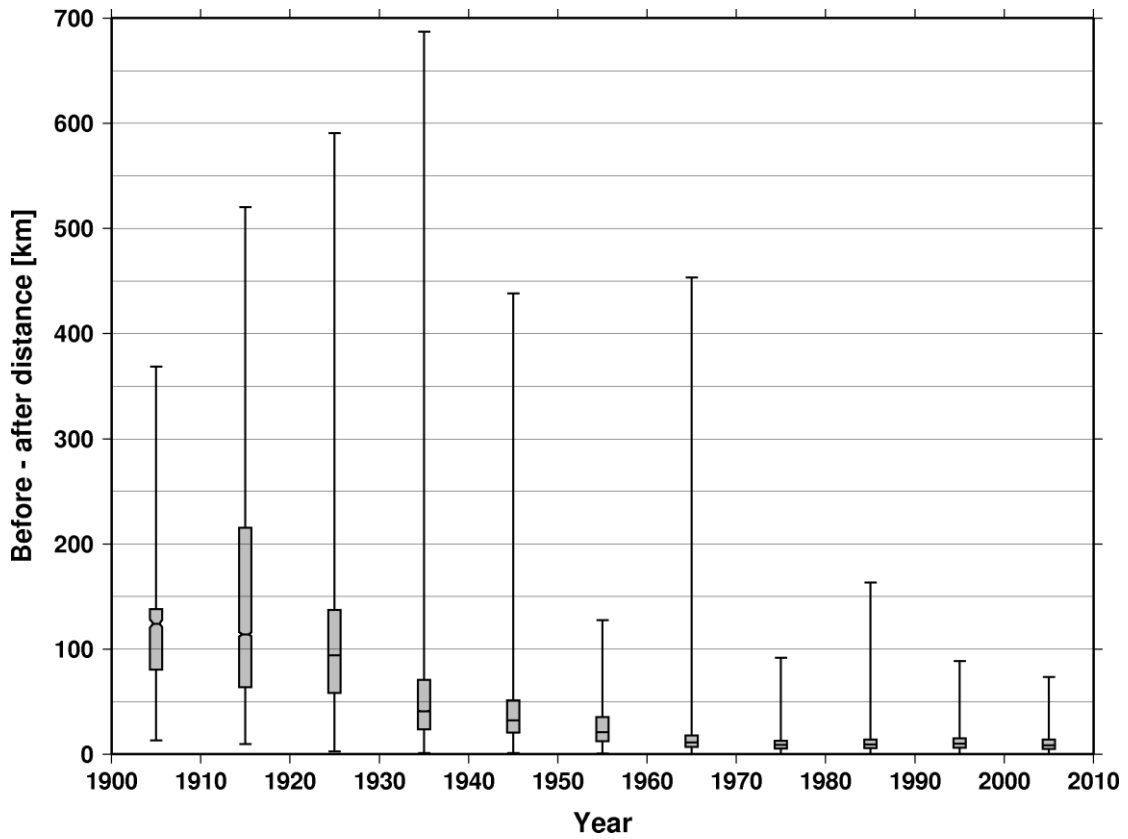


534



535

536 **Figure 8. Distribution of a) location, and b) depth differences before and after the ISC-GEM**
 537 **relocations. The 50% (median), 90% and 95% percentile points on the cumulative distributions**
 538 **(thick line) are marked with the vertical lines.**



539

540 **Figure 9. Box-and-whisker plot of the location differences before and after the ISC-GEM**
 541 **relocations in each decade. The gray boxes represent the 25% - 75% quartile ranges; the vertical**
 542 **extent of the lines indicate the full, minimum to maximum range. Event locations change the**
 543 **largest extent in the first three decades.**

544

545

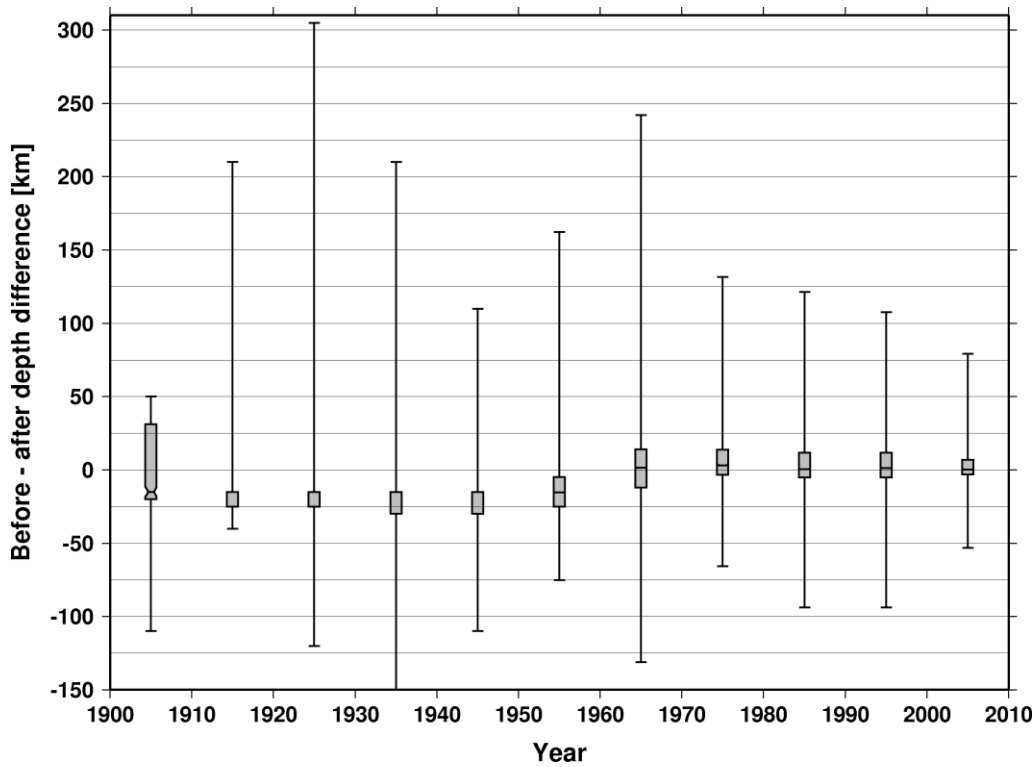
546

547

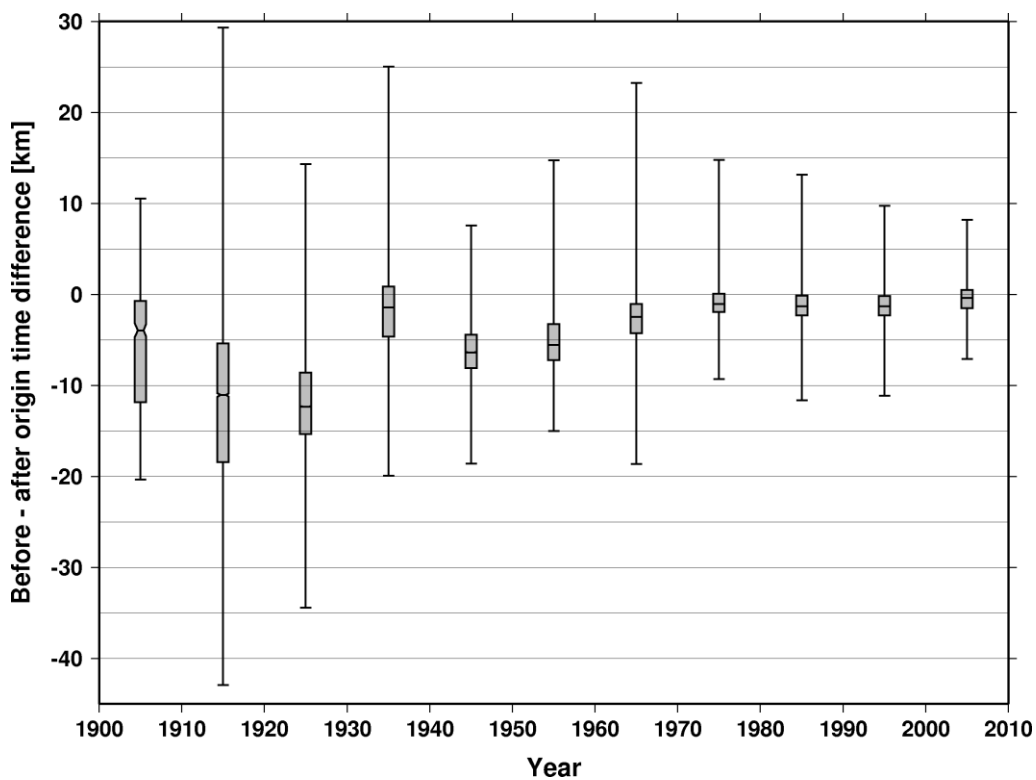
548

549

550



551



552

553 **Figure 10. Box-and-whisker plot of a) the depth, and b) origin time differences before and after**
 554 **the ISC-GEM relocations in each decade. The gray boxes represent the 25% - 75% quartile**
 555 **ranges; the vertical extent of the lines indicate the full, minimum to maximum range. The**

556 **apparent bias in the first six decades is due to the fact that previously many event depths were**
557 **fixed to the surface.**

558

559

560